The following Electronic Supplementary Information is available for this article:

Method S1: Procedure for the normalization and analysis of X-ray absorption spectroscopy data.

Method S2: Modeling procedure (Model VII).

Table S1 Initial (pCu_T) and equilibrium (pCu_{eq}) copper concentration and pH for each data point of experiment 3.

Table S2 Concentration of bound Cu (Cu_{ads}) and the proportion of each Cu ligand was derived from the best fit of the Cu K-edge extended X-ray absorption fine structure (EXAFS) spectra for wheat and tomato roots (R) and cell walls (CW), depending on the initial copper concentration (pCu_T).

Figure S1 Potentiometric titrations for wheat (squares) and tomato (circles) roots (filled symbols) and cell walls (empty symbols) expressed in charge (Q) corrected by the initial charge (Q_0).

Figure S2 Theoretical potentiometric titrations for wheat (triangles) and tomato (cross) plasma membranes expressed in charge (Q) corrected by the initial charge (Q_0).

Figure S3 Theoretical copper binding (Cu_{ads}) by wheat (triangles) and tomato (cross) plasma membranes.

Figure S4 Comparison of copper binding (Cu_{ads}) between experiment 1 (grey symbols), experiment 2 (star symbols) and 3 (colorful symbols) in wheat (a) and tomato (c) roots and wheat (b) and tomato (d) cell walls.

Figure S5 Visible shift (arrows) in the first oscillation of the Cu K-edge k^2-weighted extended X-ray absorption fine structure (EXAFS) spectra for wheat (black line) and tomato (grey line) roots, as similarly observed between the two reference compounds, i.e. Cu(II)-histidine (dotted black line) and Cu(II)-formate (dotted grey line).

Figure S6 Distribution of copper between HA_I (black line) and HA_{II} (dotted line) in wheat roots (a), cell walls (c) and plasma membranes (e) and tomato roots (b), cell walls (d) and plasma membranes (f).

Figure S7 Normalized k^2-weighted EXAFS spectra at Cu K-edge and their corresponding Fourier transform (FT) magnitudes (not corrected for phase shift) of reference compounds used to fit the roots and cell walls samples.

Method S1: Procedure for the normalization and analysis of X-ray absorption spectroscopy data.

A Cu foil was used to calibrate the X-ray energy (threshold energy taken at the zero-crossing point of the second derivative spectrum).

The data were normalized using Athena software (Ravel and Newville 2005). The k^2-weighted EXAFS (2.5 to 10.7 $Å^{-1}$) recorded on plant samples were fitted by linear combination fitting (LCF) using a library of Cu reference compounds consisting of organic and mineral species.

Principal component analysis (PCA) was applied to the EXAFS spectra to determine the number of species contained in the samples, but the PCA indicator value failed to reach a minimum. Thus, for each plant spectrum, LCFs using one, two and three reference compounds were tested successively. LCFs with n + 1 components were retained if the normalized sum-squares residual (Table S2) was decreased by more than 20% compared to the fit with n components. Satisfactory fits were obtained with a combination of two or three references. A part of the reference compound database used was described previously in Collin et al. (2014) and the compounds listed below were added. Cu(II)-gluconate, Cu(II)-phthalocyanine and libethenite (Cu_2PO_4OH) were purchased from Sigma-Aldrich. Cu(II)-galacturonate was synthesized according to the procedure of Synytsya et al. (Synytsya et al. 2004). Cu(II)-methionine and Cu(II)-phenylalanine were prepared in compliance with the protocol of Stanila et al. (2007). And Cu(II)-phytate was obtained in the same way as described in Kopittke et al. (2011).

Method S2: Modeling procedure (Model VII)

In a first step, Model VII was used to fit the potentiometric titrations previously performed by Guigues et al. (2014) on wheat and tomato roots and cell walls. These titrations were previously interpreted with the dedicated PROSECE software (Guigues et al. 2014) which enabled us, for each root material, to set the total site density as an input parameter and to give indicative values to fit the pKa_i intrinsic proton dissociation constant and the corresponding ΔpKa_i distribution term for type 1 and 2 sites. Preliminary investigations showed that it was not possible to adequately fit the titration data for tomato roots and wheat and tomato cell walls when considering single HA-type model. This was mainly due to the following condition imposed by Model VII: $L_{H1} = 2 \times L_{H2}$ (Fig. S1), constraining too much the fitting efficiency. To overcome this constraint, we fit the titration data by representing each root material with two independently parameterized HA models (HA_I and HA_{II}), i.e. low-and the high-pKa sites respectively. pKa_i. ΔpKa_i and L_{Hi} values were then optimized in order to fit the acid-base titration curves. In a second step, the Cu sorption data from experiment 3 were simulated for wheat and tomato roots and cell walls with the two HA model by optimizing the log$K_{Cu,1}$ intrinsic equilibrium constant for type-1 sites and the $\Delta LK2_{Cu,1}$ heterogeneity parameter. The log$K_{Cu,2}$ intrinsic equilibrium constant for type-2 sites was derived from log$K_{Cu,1}$ (Tipping et al. 2011):

$$logK_{Cu,2} = logK_{Cu,1} \times \frac{pKa_2}{pKa_1} \quad (1)$$

Q" Model VII can account for the complexation of the free ionic form and the first hydrolysis product of each metal, but we only accounted for Cu^{2+} as a preliminary speciation calculation showed that Cu^{2+} stood for > 99% of the total Cu in solution at pH ≤ 5.

The best fit was determined by minimizing the root mean square residual (*RMSR*), calculated as follows:

$$RMSR = \sqrt{\frac{\sum_{i=1}^{n} (x_{i,exp} - x_{i,model})^2}{n}} \quad (2)$$

where $x_{i,exp}$ is an experimental data point, $x_{i,model}$ its corresponding calculated point with the two humic-acid (HA) model and with *n* being the total number of experimental data points.

This modelling procedure was further implemented on the theoretical potentiometric titrations and Cu sorption isotherms of the outer surface of root cell plasma membranes for wheat and

tomato that were calculated according to the difference between the root and cell wall data (Figs. S2 and S3).

Table S1 Initial (pCu_T) and equilibrium (pCu_{eq}) copper concentration and pH for each data point of experiment 3.

Wheat roots			Wheat cell walls			Tomato roots			Tomato cell walls		
pCu_T	**pCu_{eq}**	**pH**	**pCu_T**	**pCu_{eq}**	**pH**	**pCu_T**	**pCu_{eq}**	**pH**	**pCu_T**	**pCu_{eq}**	**pH**
7.3	8.0	4.9	7.3	8.1	4.5	7.3	8.0	4.5	7.3	8.5	4.4
7.3	8.1	4.9	7.3	8.0	4.6	7.3	8.0	4.6	7.3	8.6	4.4
6.8	7.4	4.9	6.9	7.7	4.5	6.6	7.3	4.6	6.7	8.2	4.5
6.8	7.3	4.9	6.9	7.5	4.3	6.6	7.4	4.6	6.7	8.2	4.4
6.2	6.6	4.9	6.2	7.5	4.6	5.7	6.5	4.5	5.7	7.4	4.4
6.2	6.6	4.8	6.2	7.1	4.6	5.7	6.5	4.6	5.7	7.4	4.5
5.5	5.8	4.8	5.5	5.9	4.5	4.7	5.3	4.6	4.7	6.2	4.4
5.5	5.8	4.9	4.7	5.0	4.6	4.7	5.4	4.5	4.7	6.8	4.3
4.7	4.9	4.8	4.7	4.9	4.5	4.0	4.5	4.4	4.0	4.8	4.2
4.7	4.9	4.7	4.0	4.0	4.5	4.0	4.5	4.4	4.0	4.7	4.2
4.0	4.1	4.8	4.0	4.1	4.5	3.0	3.1	4.3	3.0	3.1	3.9
						3.0	3.2	4.1	3.0	3.1	3.9

Table S2 Concentration of bound Cu (Cu_{ads}) and the proportion of each Cu ligand was derived from the best fit of the Cu K-edge extended X-ray absorption fine structure (EXAFS) spectra for wheat and tomato roots (R) and cell walls (CW), depending on the initial copper concentration (pCu_T). The goodness of fit was assessed with the normalized sum-square (NSS) equation:

$$NSS = 100 \times \left(\sum_{i=1}^{N} [k^2\chi(k_i)_{measured} - k^2\chi(k_i)_{fitted}]^2 \right) / \left(\sum_{i=1}^{N} [k^2\chi(k_i)_{measured}]^2 \right)$$

where N is the number of points, $k^2\chi(k_i)_{measured}$ is the EXAFS spectrum of the sample in the k-space and $k^2\chi(k_i)_{fitted}$ is the EXAFS fit in the k-space.

		pCu_T	Cu_{ads} (mg.kg^{-1} initial dry roots)	Cu(II)-histidine	Cu(II)-malate	Cu(II)-malonate	Cu(II)-galacturonate	Cu(II)-acétate	Cu(II)-formate	sum	NSS (%)
Wheat	CW	6.2	66 ± 16	50			50			100	6.4
	R	6.2	113 ± 4	67			33			100	4.4
	CW	5.6	110 ± 50	61	39					100	4.2
	R	5.6	296 ± 93	73		27				100	4.7
	CW	5.2	158 ± 31	37			63			100	3.5
	R	5.2	485 ± 55	65	18	17				100	1.0
	CW	4.8	340 ± 57	65	18	17				100	1.8
	R	4.8	891 ± 20	42	58					100	2.3
Tomato	CW	6.2	61 ± 1	55					45	100	6.4
	R	5.9	80 ± 24	56					44	100	6.9
	CW	5.6	226 ± 27	42		20			38	100	5.5
	R	5.6	270 ± 40	51					49	100	7.0
	R	5.2	658 ± 88	57				43		100	5.3

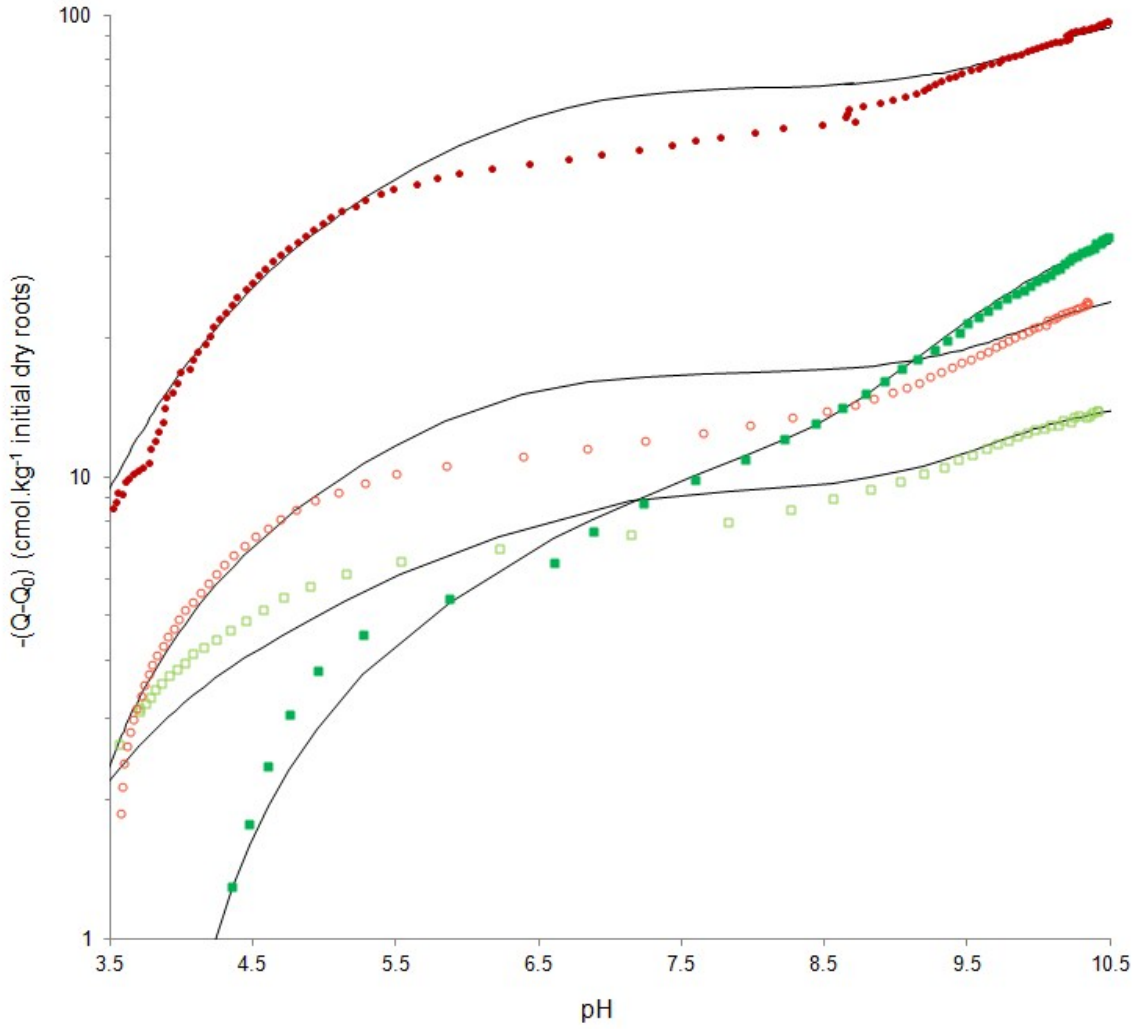

Figure S1 Potentiometric titrations for wheat (squares) and tomato (circles) roots (filled symbols) and cell walls (empty symbols) expressed in charge (Q) corrected by the initial charge (Q_0). Solid lines refer to the fitting curves obtained with model VII using one humic-acid, as described in the Material and Methods.

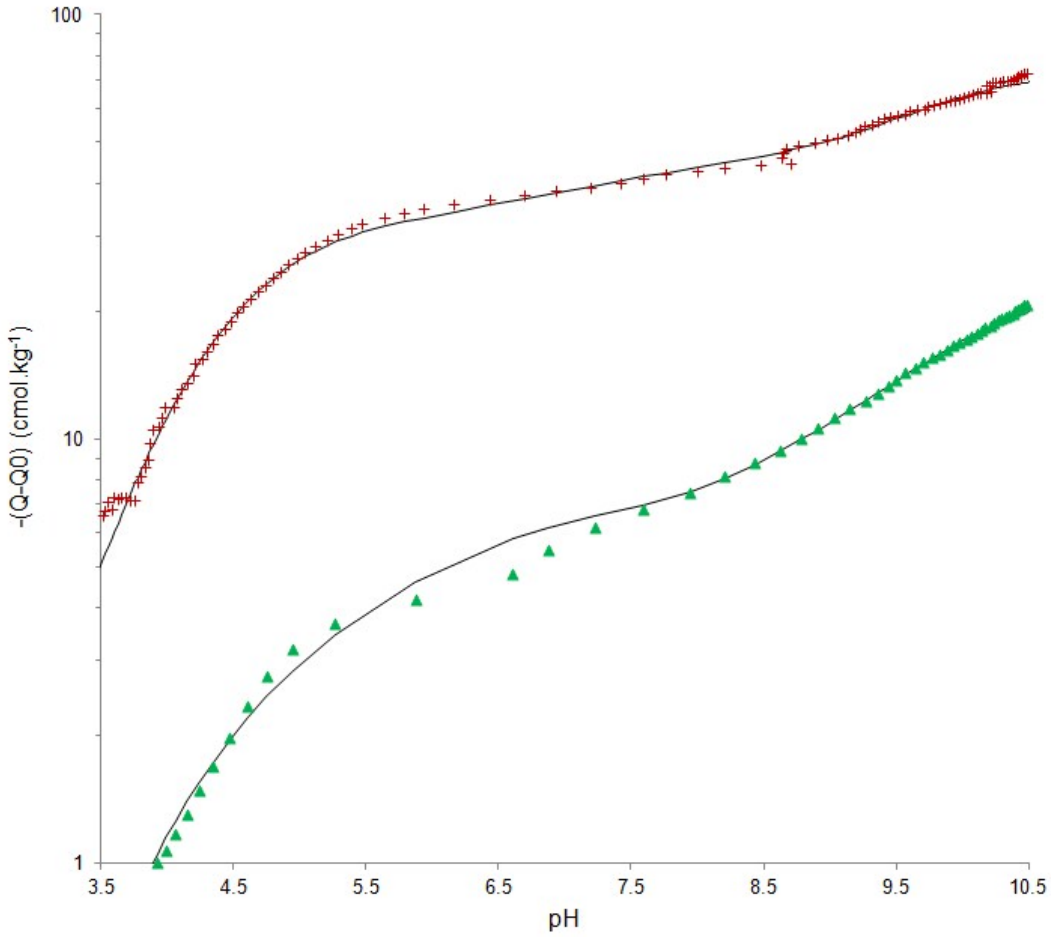

Figure S2 Theoretical potentiometric titrations for wheat (triangles) and tomato (cross) plasma membranes expressed in charge (Q) corrected by the initial charge (Q_0). Solid lines refer to the fitting curves obtained with model VII using the two HA model as described in the Material and Methods.

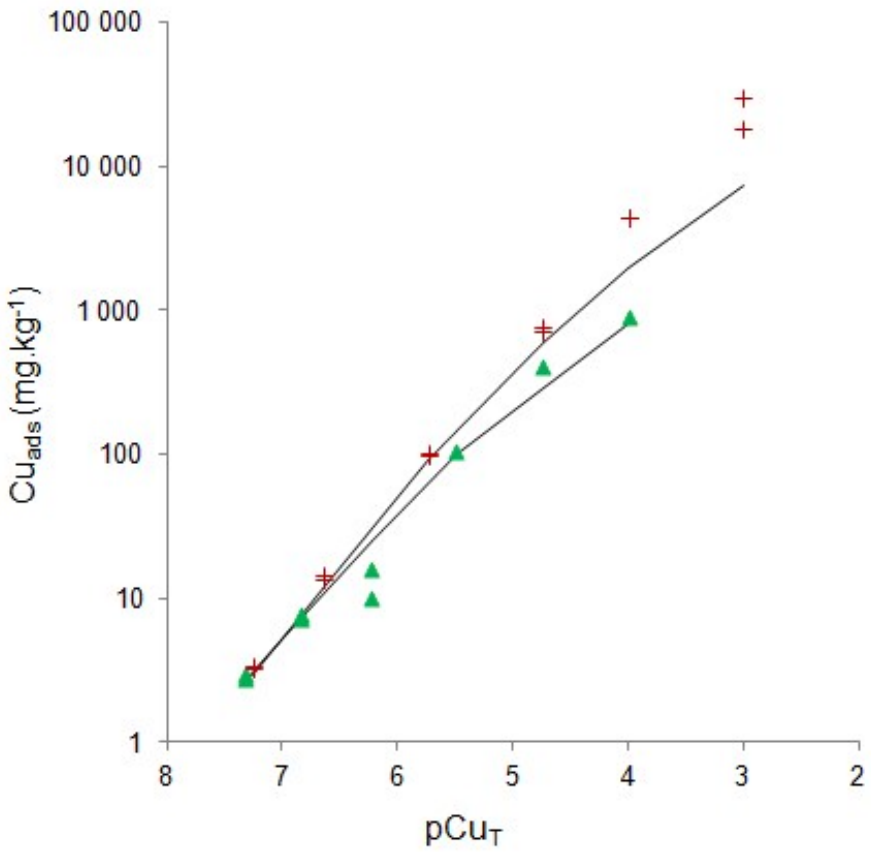

Figure S3 Theoretical copper binding (Cu_{ads}) by wheat (triangles) and tomato (cross) plasma membranes. Solid lines refer to the fitting curves obtained with the two HA model as described in the Material and Methods.

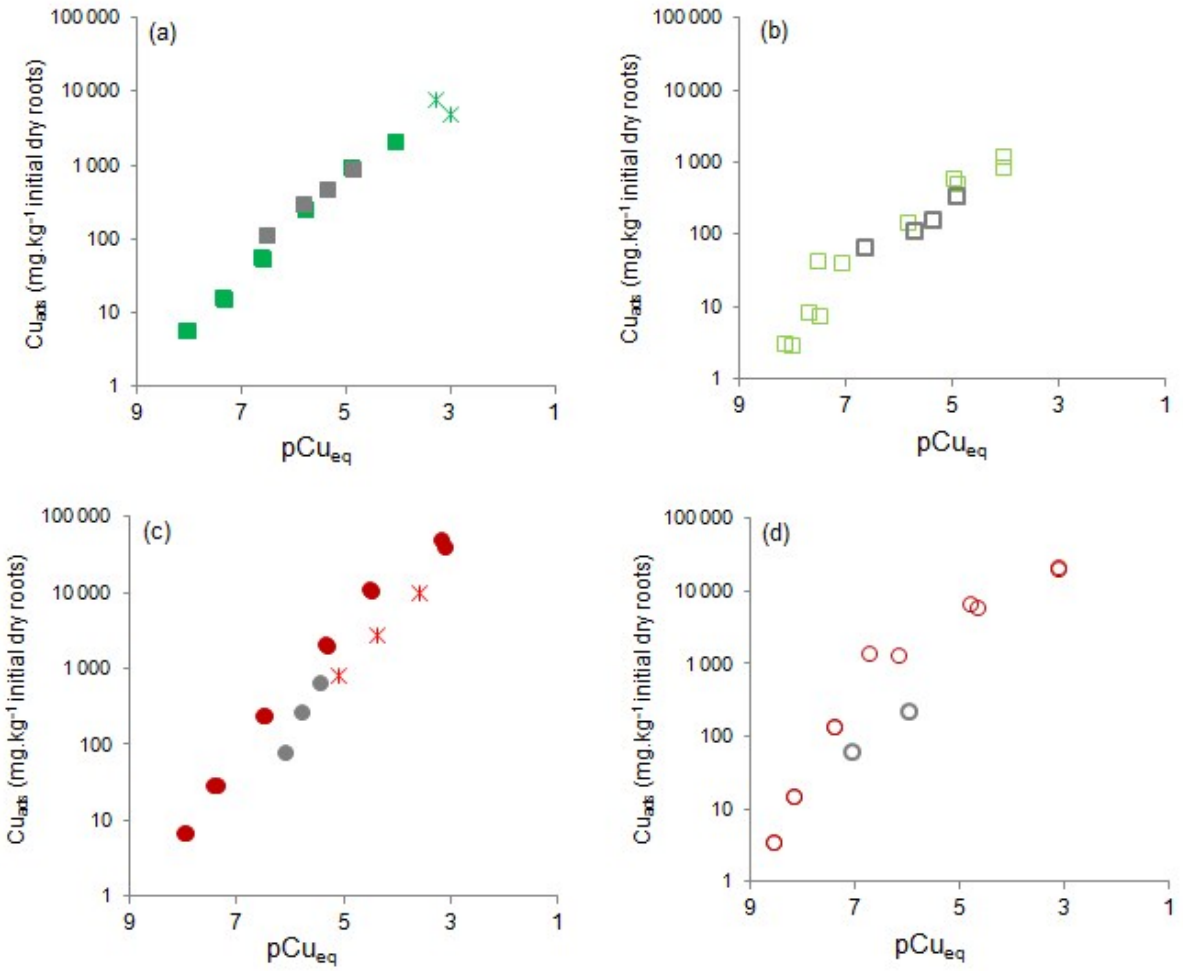

Figure S4 Comparison of copper binding (Cu_{ads}) between experiment 1 (grey symbols), experiment 2 (star symbols) and 3 (colorful symbols) in wheat (a) and tomato (c) roots and wheat (b) and tomato (d) cell walls.

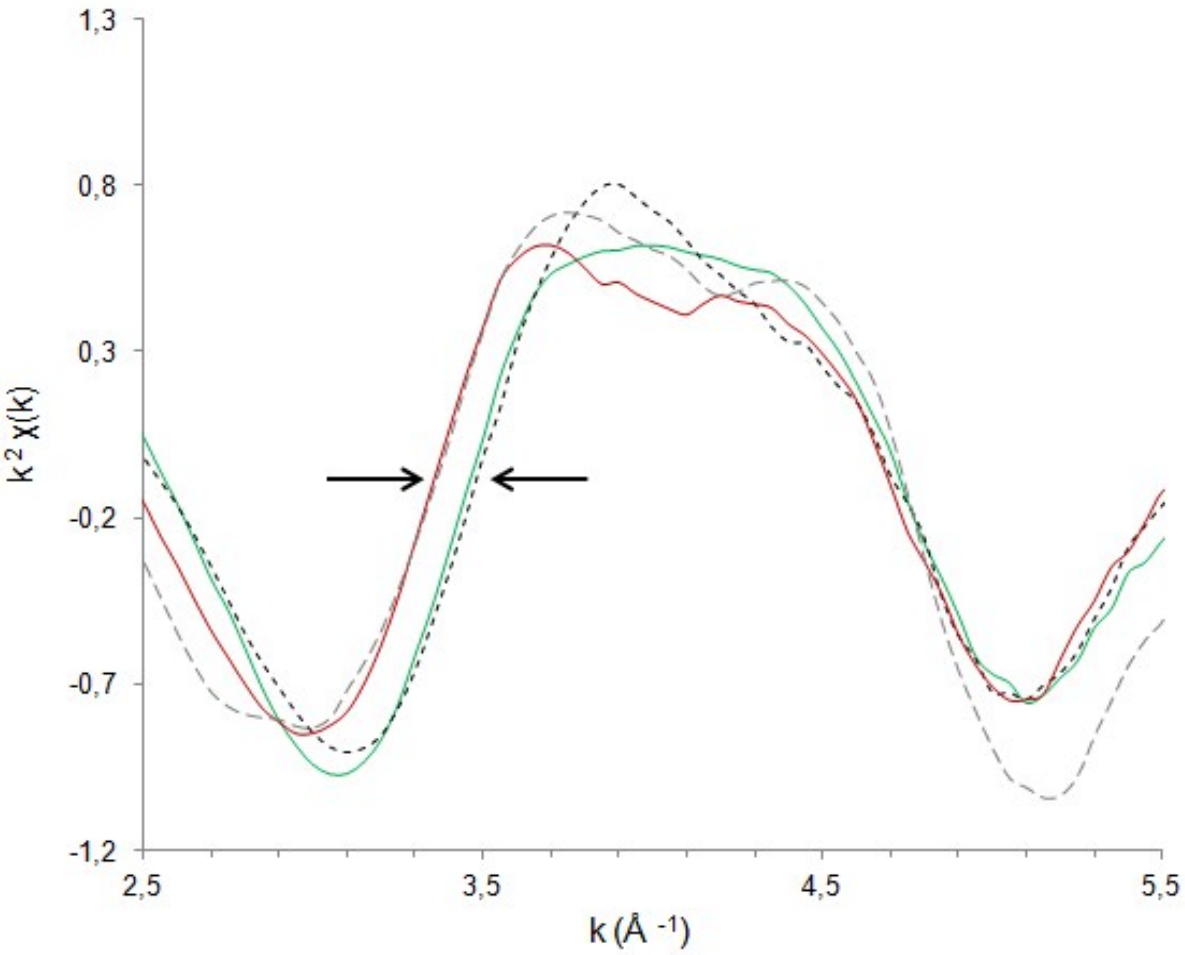

Figure S5 Visible shift (arrows) in the first oscillation of the Cu K-edge k^2-weighted extended X-ray absorption fine structure (EXAFS) spectra for wheat (green line) and tomato (red line) roots, as similarly observed between the two reference compounds, i.e. Cu(II)-histidine (dotted black line) and Cu(II)-formate (dotted grey line).

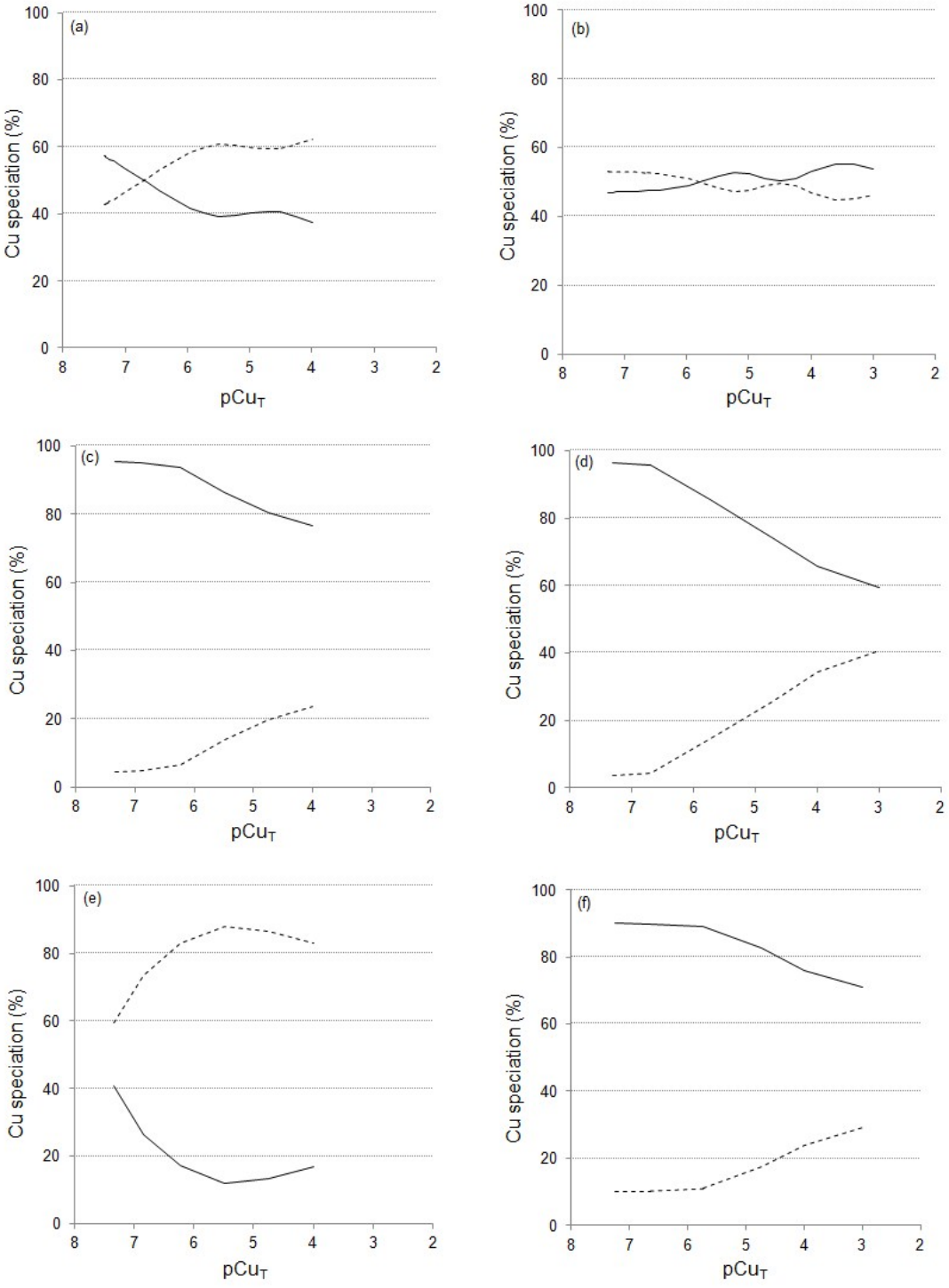

Figure S6 Distribution of copper between HA_I (black line) and HA_{II} (dotted line) in wheat roots (a), cell walls (c) and plasma membranes (e) and tomato roots (b), cell walls (d) and plasma membranes (f).

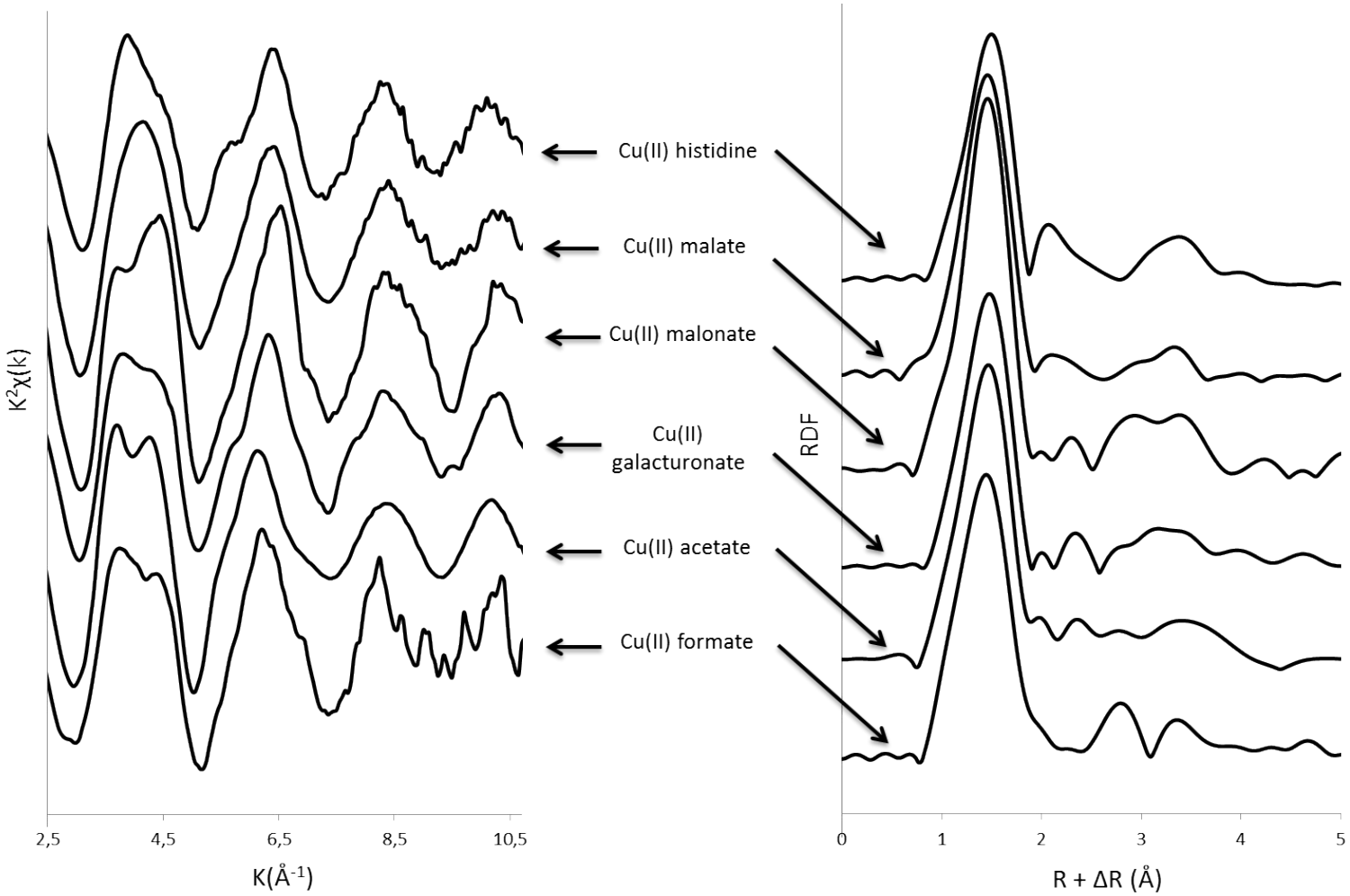

Figure S7 Normalized k^2-weighted EXAFS spectra at Cu K-edge and their corresponding Fourier transform (FT) magnitudes (not corrected for phase shift) of reference compounds used to fit the roots and cell walls samples.

References

Collin B et al. (2014) Evidence of sulfur-bound reduced copper in bamboo exposed to high silicon and copper concentrations. Environ Pollut 187:22-30. doi:http://dx.doi.org/10.1016/j.envpol.2013.12.024

Guigues S, Bravin M, Garnier C, Masion A, Doelsch E (2014) Isolated cell walls exhibit cation binding properties distinct from those of plant roots. Plant Soil 381:367-379. doi:10.1007/s11104-014-2138-1

Kopittke PM et al. (2011) In Situ Distribution and Speciation of Toxic Copper, Nickel, and Zinc in Hydrated Roots of Cowpea. Plant Physiol 156:663-673. doi:10.1104/pp.111.173716

Ravel B, Newville M (2005) ATHENA, ARTEMIS, HEPHAESTUS: data analysis for X-ray absorption spectroscopy using IFEFFIT. J Synchrotron Rad 12:537-541

Stanila A, Marcu A, Rusu D, Rusu M, David L (2007) Spectroscopic studies of some copper(II) complexes with amino acids. J Mol Struct 834–836:364-368. doi:http://dx.doi.org/10.1016/j.molstruc.2006.11.048

Synytsya A et al. (2004) The complexation of metal cations by d-galacturonic acid: a spectroscopic study. Carbohydr Res 339:2391-2405. doi:http://dx.doi.org/10.1016/j.carres.2004.07.008

Tipping E, Lofts S, Sonke JE (2011) Humic Ion-Binding Model VII: a revised parameterisation of cation-binding by humic substances. Environ Chem 8:225-235. doi:10.1071/en11016